PROCEEDINGS of the
23rd International Congress on Acoustics

9 to 13 September 2019 in Aachen, Germany

Research on Aerodynamic Noise Calculation and Noise Reduction Design of Multi-blade Centrifugal Fan

Jinan HUANG[1]; Yang XIANG[2]; Chaojun JIANG[3]

[1] Wuhan University Of Technology, China

[2] Wuhan University Of Technology, China

[3] Wuhan University Of Technology, China

ABSTRACT

Taking the multi-blade centrifugal fan in an air-conditioning system as the object, the three-dimensional modeling of the internal fluid of the fan is carried out. The steady-state and non-steady-state calculations are carried out in the CFD software, obtaining the internal flow field information, with the calculation result imported into noise estimation which was performed in the LMS Virtual.lab. Besides, the accuracy of the fan aerodynamic noise calculation was verified against the experimental results. Through the analysis of the mechanism of the aerodynamic noise of the fan, the main noise source of the aerodynamic noise of the fan is located at the impeller and is closely related to its internal flow field distribution and its structure. For the fan products that have been put into production, it is difficult to modify the main structure including the volute, the impeller, the blade size, etc., and only local structure can be redesigned to achieve the purpose of noise reduction. Therefore, the blade perforation design is adopted. By setting reasonable perforation parameters, the eddy current shedding around the blade can be reduced without changing its performance, so as to reduce the pressure pulsation of the blade surface and the aerodynamic noise of the fan.
Keywords: Centrifugal Fan; Aerodynamic Noise; Blade Perforation

1. INTRODUCTION

The air conditioning system fan has the problems of large vibration and high noise, but in order to ensure the good air circulation, the fan needs to ensure efficient operation at all times. Continuous noise can make people feel upset and unable to concentrate, and in severe cases, it can cause harm to people's hearing, vision, nervous system and so on. Studying the causes of fan noise and its prevention methods are of great significance to improve the quality of the work environment.

Due to the complexity of the flow field dynamics of the fan and the limitation of experimental cost and conditions, the flow field simulation of the fan based on CFD theory is gradually adopted, which becomes an important means to figure out the optimization of the flow field and noise estimation of the fan. Carlos Pérez Arroyo[1]explained the mechanism of fan noise generation. Literature[2~4]accurately predicted the noise of uneven blade fan and made noise reduction design from the structural point of view. Subagyo[5]made an accurate calculation of the optimized fan noise.Alexej Pogorelov[6] introduced in detail the calculation method of flow field and sound field of axial flow fan.Sheryl[7] compared the broadband noise of different fan models For the fan products that have been put into production, it is difficult to make major changes to its main structure.This paper explores the use of blade perforation design, by setting reasonable perforation parameters, reducing the eddy current shedding around the blade under the condition that the fan performance is basically unchanged, so as to reduce the pressure pulsation of the blade surface to reduce the aerodynamic noise of the fan, and provide a method for fan noise reduction reference.

2. MODEL BUILDING AND MESHING

The fan of this paper is a multi-blade centrifugal fan of an air-conditioning system. The structure

[1] 1075175743@qq.com
[2] yxiang@whut.edu.cn
[3] 853958641@qq.com

is mainly composed of impeller, volute and wind collector. Create a 3D physical model in Solidworks as shown below.

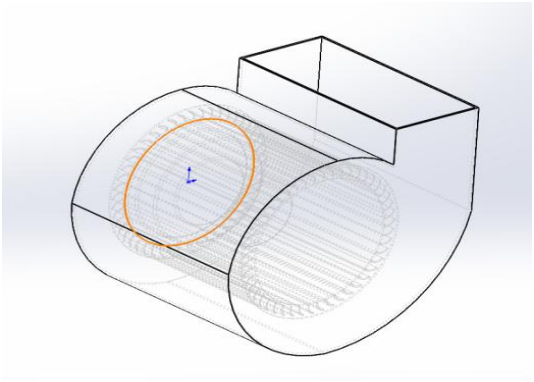

Figure 1 Basic structure of the fan model

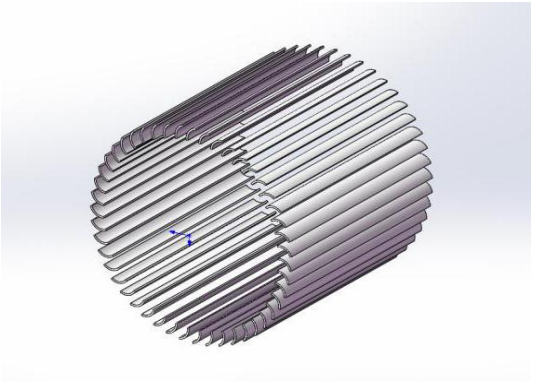

Figure 2 Blade physical model

The basic parameters are shown in Table 1.

Table 1 Basic parameters of the fan

Rotating speed (rpm)	Number of blades	Outer diameter of the impeller (mm)	Inner diameter of the impeller (mm)	Diameter ratio	Impeller length (mm)	Volute width (mm)
960	47	260	214	0.82	254	306

Based on the structural model, the internal fluid model of the fan is established, and it is meshed by ANSYS ICEM. The automatic body mesh, that is, the unstructured mesh is used to divide the tetrahedral mesh. In this paper, the frequency is about 3500 Hz. Under the condition that there are at least 6 units in a single wavelength, the mesh is encrypted at the impeller, blade and their interface. The total number of meshes is 8801375.

3. Flow field simulation

3.1 Calculation parameter settings

The multi-reference system model is used to simulate the internal flow path of the fan, and the flow field and the static field are solved simultaneously. The flow field information of the two sub-areas is transmitted through the shared interface and affect each other. The moving zone and the quiet zone adopt different coordinate systems, the moving zone adopts a rotating coordinate system, and the quiet zone is a stationary coordinate system. The impeller area and the central area are defined as the rotating area, and the rotating coordinate system is used, and the fluid is given a corresponding rotating speed.

Although the target fluid is air, it can be regarded as an incompressible gas due to its change in the negligible density in this environment. The selection of the turbulence model is due to the equivalent diameter of 0.188 m at the nozzle and the Reynolds number of 431891. A full turbulent Reynolds number far greater than 4000. Therefore, the k-ε standard turbulence model is selected, and the model is only effective for the high Reynolds number flow field model which is completely turbulent. Select the entry for standard initialization and perform 1500 iterations until convergence.

3.2 Flow field result analysis

3.2.1 Velocity field result

The axial speed streamline diagram of the fan is shown in Figure 3. At the corner of the impeller exit near the fan rear disk area, due to the sudden expansion of the flow path area, two vortex areas with opposite rotation directions appear; due to the influence of centrifugal force, A region near the inside of the volute forms a secondary flow; on the side near the exit of the volute, there is also a

vortex region in the front disk region behind the intake port. From the radial velocity cloud analysis of the fan in Figure 4, the flow velocity increases near the surface of the fan impeller and near the bottom of the impeller and the volute, and the velocity distribution is not symmetrical as a whole. The asymmetry of this flow may be caused by the asymmetry of the volute shell structure.

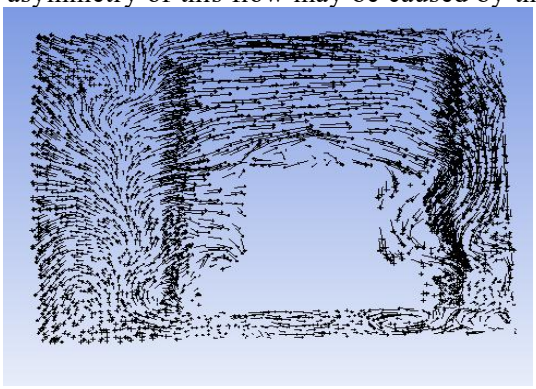

Figure 3 Axial velocity streamline diagram

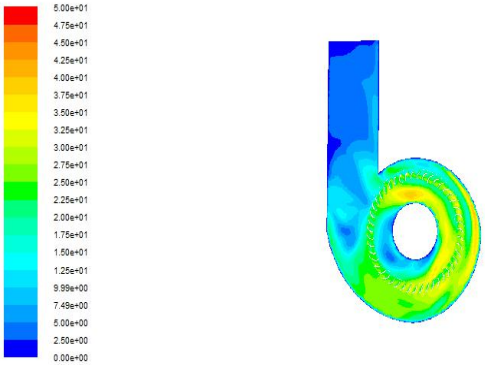

Figure 4 Radial velocity distribution

3.2.2 Pressure field result

From the radial pressure cloud diagram of the fan in Fig. 5 and the pressure distribution on the blade surface of Fig. 6, it is known that the inner surface of the impeller has a small pressure rise near the shaft, the pressure near the inner surface of the volute is higher than the inside of the volute, and the pressure of the outlet pipe gradually increases along the exit direction. rise. The impeller rotates to work on the inflowing gas, and the impeller increases from the inlet to the outlet. The impeller and the vane rotate in a clockwise direction, the outer surface pressure is slightly greater than the inner surface pressure, and the closer the relative position is to the volute, the greater the pressure.

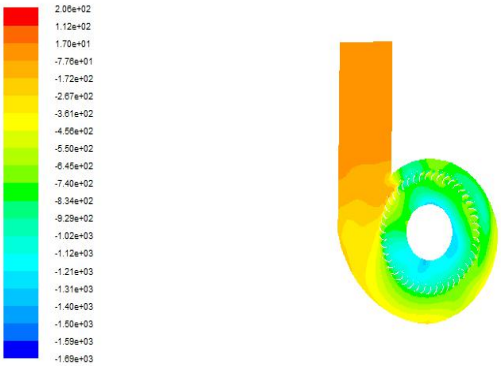

Figure 5 Radial pressure distribution

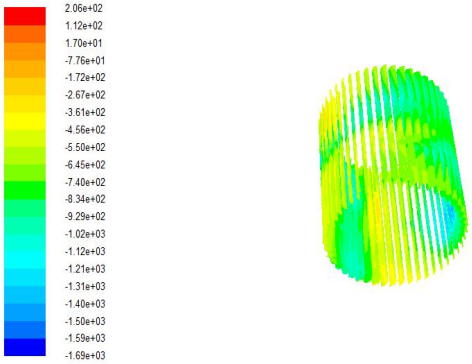

Figure 6 Leaf surface pressure distribution

4. Fan noise prediction and noise reduction research

4.1 Noise prediction

Based on the steady state results of the flow field, the large-eddy simulation LES is used to calculate the transient results of the flow field, and then the transient flow field result is imported into the CGNS file form, but the sound field of the fan is calculated in the acoustic software of LMS Virtua.lab. The noise simulation uses the noise comparison model FW-H[8]. According to the derivation process of the Lighthill equation, the FW-H equation can be derived:

$$\frac{1}{c_0^2}\frac{\partial^2 p'}{\partial t^2}-\frac{\partial^2 p'}{\partial x_i^2}=\frac{\partial}{\partial t}[\rho_0 v_j \eta_j \delta(f)]-\frac{\partial}{\partial x_i}[p_{ij}\eta_j\delta(f)]+\frac{\partial^2 T_{ij}}{\partial x_i \partial x_j} \quad (1)$$

Where:c_0——the far field sound velocity; p'——the sound pressure at the observation point; $x_i x_i$——the two coordinate components of the control plane; ρ_0——density; η_i——the normal vector outside the control plane; v_i——the speed of the control plane; $\delta(f)$——Dirac function; p_{ii}——Stress tensor; T_{ii}—— Lighthill tensor.

From the classification and summary of the mechanical aerodynamic noise source of the impeller, it is divided into a monopole noise source, a dipole noise source and a quadrupole noise source[9].

The monopole noise source (blade thickness noise) is not the main noise source of the turbomachine, and its noise radiation level is not large and can generally be ignored. In addition, from the basic theory of aerodynamic noise, the acoustic intensity of the kinetic radiation noise of the dipole is proportional to the sixth power of the fluid velocity, while the acoustic intensity of the pulsating stress of the quadrupole radiates noise and the eighth power of the fluid velocity. In proportion, the experimental measurements further show that the random noise of the impeller is proportional to the flow velocity of the sixth power. Therefore, the random acoustic radiation generated by the quadrupole pulsation stress can be neglected compared with the acoustic radiation generated by the pulsating pressure of the dipole.

The selected blade model is imported into virtual.Lab, and the fan sound source is defined. Since the blade length is 254 mm, the blade is equivalent to the rotating dipole, and the size needs to be smaller than the acoustic wavelength, so as shown in Figure7. Each blade is divided into 15 segments, each segment being equivalent to a source of 16.9 mm.

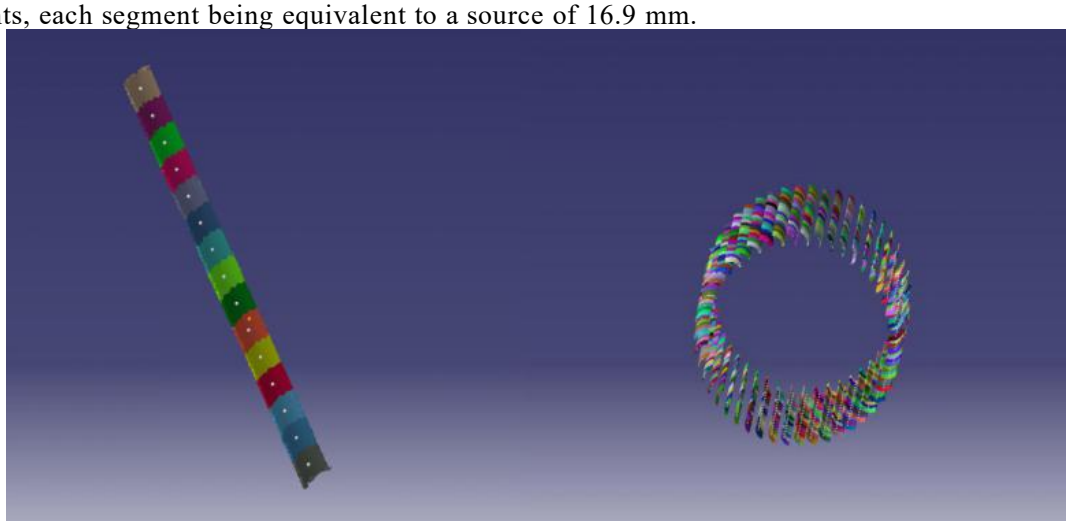

Figure 7 Blade segmentation applied dipole

The simulation field is set at a distance of 1 m from the center of the fan to calculate the fan noise, and another monitoring point is set at 0.45 m from the axial center of the fan to calculate the fan radiated noise.

4.2 Noise estimation result analysis

Table 2 shows the calculated sound pressure value of the fan under different working conditions and the measured sound pressure value of the fan manufacturer. It can be seen that under the influence of the actual environment and manual operation, the error between the simulated data and the measured value is within 2 dB. It shows that the simulation method is basically reliable in this process.

Table 2 Fan noise comparison

Q （m^3/h）	1547	1815	2101	2352	2587
Noise calculation （dB）	59.68	60.76	62.24	63.35	64.08
Noise measured value （dB）	58	59	60.5	62	62.5

The blade passing frequency BPF=N*r/60, where ‘N’ is the number of blades rotor 47, ‘r’ is the speed 960r/min, and the calculated blade fundamental frequency is 752HZ. Figure 7-10 shows the sound pressure distribution of the field point and the sound pressure distribution on the surface of the volute at the blade passing frequency and its harmonic frequencie. The sound field point is directly above the fan exit direction. At 752HZ, the sound pressure is rapidly attenuated along the exit pipe. Ineffectively propagates along the direction of the outlet pipe. As the frequency increases, the sound pressure gradually propagates outward. This is because when the pipe section is large or the sound frequency is high, the sound propagation path will change, not completely along the pipe axis spread. At each frequency, the sound pressure value of the part near the impeller and the volute is generally higher than other positions, which is closely related to the steady flow field distribution at the intersection of the impeller and the volute.

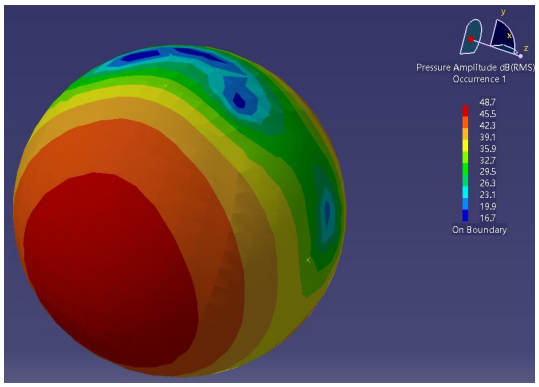

Figure 7 (752Hz) field sound pressure

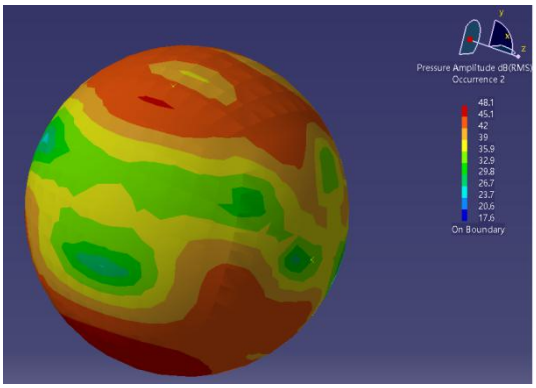

Figure 8 (1504Hz) field sound pressure

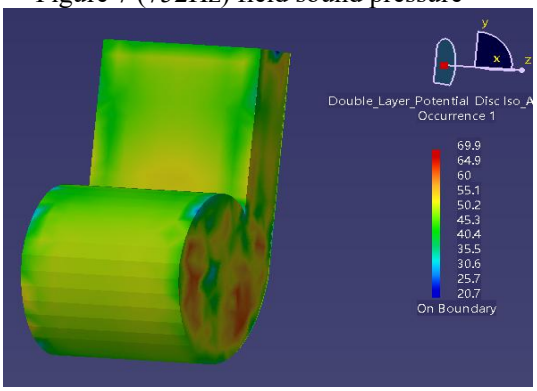

Figure 9 (752Hz) volute surface sound pressure

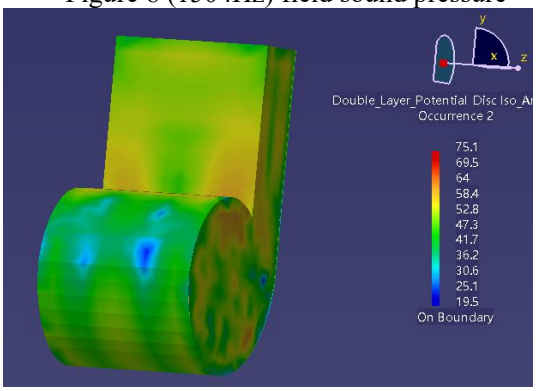

Figure 10 (1504Hz) volute surface sound pressure

4.3 Fan noise reduction design

In order to reduce the eddy current noise of the fan, the method of blade perforation is adopted to reduce and suppress the generation of eddy current detachment. In this paper, the fan blade width is 20mm, and 15 holes with a diameter of 3mm are evenly distributed on the blade axis. The design is to reduce the influence of structural asymmetry on noise, and at the same time reduce the impact of the aerodynamic performance of the fan as much as possible. Adopting a small aperture design also ensures that the blade does not suffer from insufficient strength. The final perforation model is shown in Figure 11:

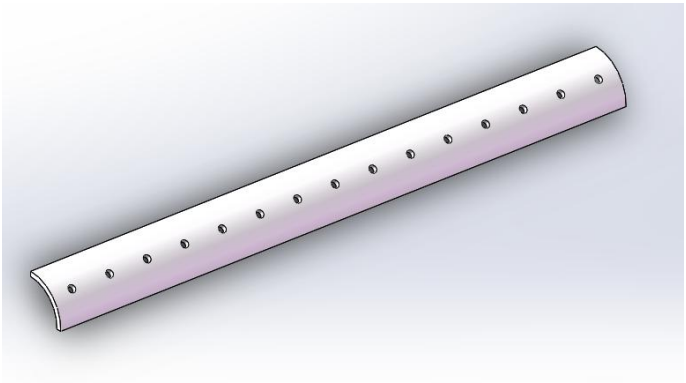

Figure 11 Blade perforation model

Repeat the above method and process to calculate the flow field and noise of the fan after piercing. Figure 12 is a streamline diagram of the vortex intensity of the fan before and after the perforation. By comparison, it is found that the partial airflow of the blade perforation flows directly from the working surface to the non-working surface, so that the boundary velocity distribution of the non-working surface is improved, and the occurrence of eddy current detachment is suppressed. The turbulence intensity in the exhaust runner after the perforation of the fan is significantly lower than that before the perforation. The turbulence intensity of the section before perforation is in the range of 21.3~53.2, while the turbulence intensity of the section after perforation is mostly less than 21.3. It can be seen that the perforation of the fan blades reduces the turbulence intensity of the airflow.

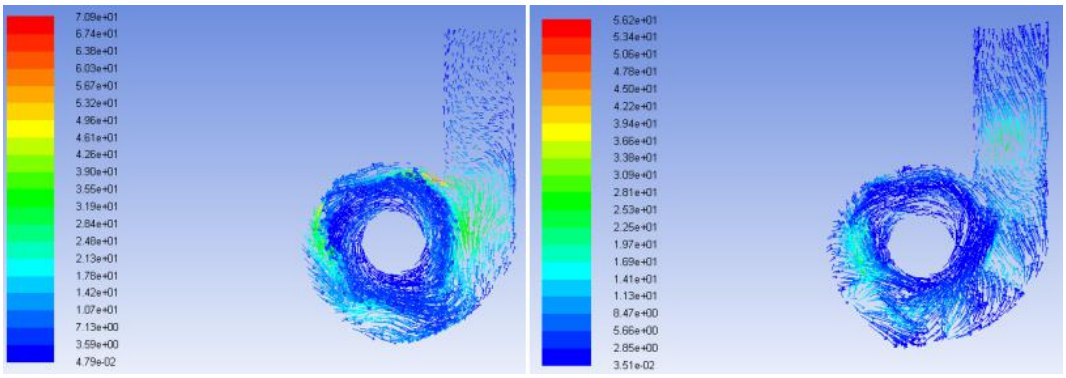

Figure 12 Eddy current intensity streamline diagram before and after perforation

Figure 13 is a comparison of the sound pressure level spectrum of the monitoring points before and after the perforation. The trend of the sound pressure spectrum of the monitoring points before and after the perforation is basically the same, and the noise of the fan after perforation is significantly reduced.

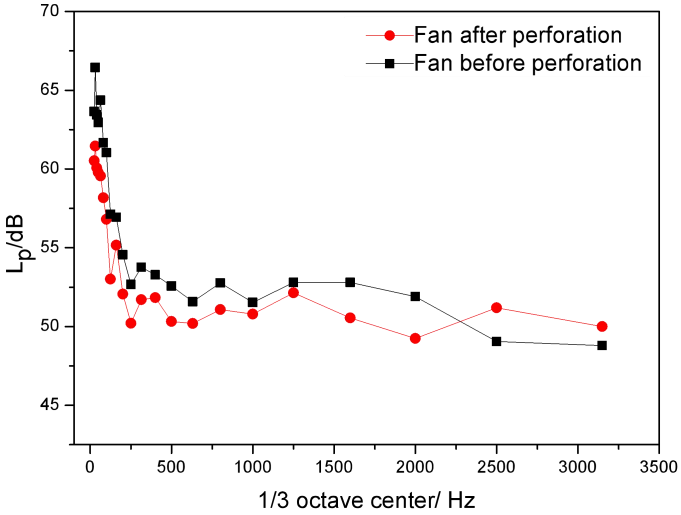

Figure 13 Monitoring sound pressure before and after perforation

Table 3 shows a comparison of the sound pressure levels before and after the 1/3 octave center frequency point is punched. It can be more intuitively seen that after the fan is pierced, the A sound level can be reduced by 3~5dB, and the overall noise of the fan can be reduced to below 60dB. Although there is an increase at 2500 Hz and 3150 Hz, the sound pressure level is lower in the range of 2500 Hz to 3150 Hz, which has less effect on the total sound level of the fan. The reason for the increase in noise in the high frequency band is that airflow regenerating noise is generated when the working surface airflow flows through the small holes after the perforated blades are used. Reasonable optimization of perforation parameters can effectively suppress airflow regeneration noise.

Table 3 Sound pressure comparison

Center frequency (Hz)	31.5	63	125	250	500	800	1000	1250	2000	2500	3150
Original fan(dB)	66.44	64.37	57.13	52.67	52.58	52.77	51.52	52.80	51.90	49.04	48.80
Perforated blade fan(dB)	61.46	59.56	53.01	50.21	50.32	51.08	50.79	52.13	49.24	51.19	50.00

At the same time, the performance of the fan before and after the perforation is compared. From

the flow-static pressure curve of the fan before and after the perforation in Figure 14, it can be seen that the static pressure of the two models decreases with the increase of the flow rate in the whole watershed; After perforation, part of the gas does not work through the rotor, resulting in a smaller static pressure rise than the prototype fan, but at the design operating point Q = 2101 m3 / h, the pressure difference between the two fan models is basically the same. Figure 15 shows the flow-efficiency curve of the fan before and after the perforation. It can be seen that the two fan models have the same trend in the working flow range. The efficiency increases first and then decreases with the increase of the flow rate. After the perforation, the working efficiency of the model decreased slightly overall, but in the vicinity of the best operating point, the efficiency values of the two models reached the maximum and the difference was only 0.4%. The model after perforation can meet the actual working requirements.

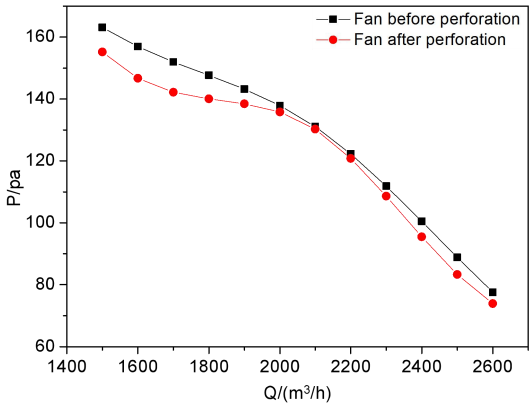

Figure 14 Flow-static pressure curve

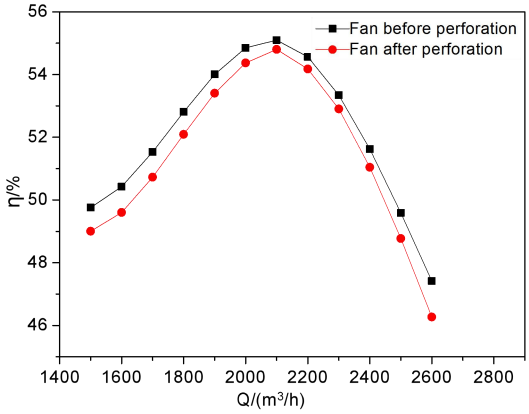

Figure 15 Flow-efficiency curve

5. CONCLUSIONS

According to the numerical calculation results, the flow field law of the fan is analyzed, and the causes of the aerodynamic noise of the fan are summarized. The accuracy of the calculation method is verified by comparison with experimental values of sound pressure. Comparing the sound pressure level, flow-static pressure relationship and flow-efficiency relationship of the fan monitoring points before and after the blade perforation design, the following conclusions are drawn:

a) Fan noise is closely related to the intensity and quantity of eddy current in the flow field. The fluid flows from the working surface of the blade to the non-working surface. Due to the speed difference, a large number of eddy currents are generated at the edge of the blade, resulting in an increase in fan noise.

b) After the perforation of the blade, part of the airflow flows directly from the working surface to the non-working surface, so that the boundary velocity distribution of the non-working surface is improved, and the occurrence of eddy current detachment is suppressed. The turbulence intensity in the exhaust runner after the fan is perforated is significantly lower than that before the piercing, so the fan noise is significantly improved compared with the previous one.

c)Although the static pressure and efficiency are smaller than the prototype fan after the blade is perforated, the pressure and efficiency differences of the two fan models are small in the vicinity of the design operating point. The fan performance can be minimized by further optimizing the perforation parameters. Therefore, under the condition that the performance of the fan is reduced, the reasonable perforation design can effectively reduce the fan noise.

ACKNOWLEDGEMENTS

The research is supported in part under the National Natural Science Foundation of China (project nos. 51279148).

REFERENCES

1. Carlos Pérez Arroyo,Thomas Leonard,Marlene Sanjose,Stéphane Moreau,Florent Duchaine. Large Eddy Simulation of a scale-model turbofan for fan noise source diagnostic[J]. Journal of Sound and Vibration,2019.

2. Yadong Wu,Dinghao Pan,Zhigang Peng,Hua Ouyang. Blade force model for calculating the axial noise of fans with unevenly spaced blades[J]. Applied Acoustics,2019,146.
3. Seung Joong Kim,Hyung Jin Sung,Stefan Wallin,Arne V. Johansson. Design of the centrifugal fan of a belt-driven starter generator with reduced flow noise[J]. International Journal of Heat and Fluid Flow,2019,76.
4. Boyan Jiang,Jun Wang,Xiaopei Yang,Wei Wang,Yanyan Ding. Tonal noise reduction by unevenly spaced blades in a forward-curved-blades centrifugal fan[J]. Applied Acoustics,2019,146.
5. Subagyo. Noise prediction on the design of optimized fan by numerical simulation[J]. Journal of Physics: Conference Series,2018,1130(1).
6. Alexej Pogorelov, Mehmet Onur Cetin,Seyed Mohsen Alavi Moghadam,Matthias Meinke,Wolfgang Schröder. Aeroacoustic Simulations of Ducted Axial Fan and Helicopter Engine Nozzle Flows[M].Springer International Publishing:2016-06-15.
7. Sheryl M. Grace,Michaela M. Logue. Comparison of two low-order models for the prediction of fan broadband noise[J]. Journal of Sound and Vibration,2018,431.
8. R. M. Orselli,B. S. Carmo,J. R. Meneghini,R. L. Queiroz,A. S. Bonatto. Noise Predictions of the Advanced Noise Control Fan Using a Lattice Boltzmann Method and Ffowcs Williams-Hawkings Analogy[M].Springer International Publishing:2015-06-15.
9. Heinrich Kuttruff. Acoustics[M].Taylor and Francis:2014-05-29.